Time-of-Flight Measurements as a Possible Method to Observe Anyonic Statistics

R. O. Umucalılar,[1] E. Macaluso,[2] T. Comparin,[2] and I. Carusotto[2]
[1]*Deparment of Physics, Mimar Sinan Fine Arts University, 34380 Sisli, Istanbul, Turkey*
[2]*INO-CNR BEC Center and Dipartimento di Fisica, Università di Trento, 38123 Povo, Italy*

(Received 24 December 2017; published 6 June 2018)

We propose a standard time-of-flight experiment as a method for observing the anyonic statistics of quasiholes in a fractional quantum Hall state of ultracold atoms. The quasihole states can be stably prepared by pinning the quasiholes with localized potentials and a measurement of the mean square radius of the freely expanding cloud, which is related to the average total angular momentum of the initial state, offers direct signatures of the statistical phase. Our proposed method is validated by Monte Carlo calculations for $\nu = 1/2$ and $1/3$ fractional quantum Hall liquids containing a realistic number of particles. Extensions to quantum Hall liquids of light and to non-Abelian anyons are briefly discussed.

DOI: 10.1103/PhysRevLett.120.230403

Introduction.—The usual exchange statistics, which classifies particles into bosons and fermions, is enriched in two dimensions (2D). In 2D, the many-particle wave function can, in principle, acquire an arbitrary statistical phase factor $\exp(i\phi_{\mathrm{st}})$ upon particle exchange, which can be different from the usual ± 1 factor defining bosons and fermions [1,2]. Particles having this unusual fractional exchange statistics are called anyons [3]. In the presence of topologically degenerate ground states, the phase factor when anyons are braided around each other can even be replaced by non-Abelian transformations acting on the ground state manifold [4], with interesting potential applications in topological quantum computing [5].

Among the 2D systems where anyons appear naturally, fractional quantum Hall (FQH) systems are, perhaps, the most commonly studied ones [3,6,7]. Quasihole and quasiparticle excitations of an FQH system are known to exhibit anyonic character [8]. Although the FQH effect was originally observed in 2D electron gases under a magnetic field [9], analogue systems where interacting neutral particles experience synthetic magnetic fields [10,11] are emerging as promising platforms for studying FQH physics. Ultracold atomic [12] and photonic systems [13], being prime examples of such analogue systems, are advantageous over the electronic ones in that they offer a highly controllable environment. In these systems, it might be possible to pin and braid anyons using localized potentials for particles [14–17].

While the fractional charge of (Abelian) anyons in FQH systems has been experimentally observed via shot-noise measurements [18], no clear-cut evidence of the exchange statistics is yet available. Although interferometric measurements performed, so far, in electronic systems are highly suggestive of anyonic statistics [19], they still lack a unique interpretation [20]. More recent studies on the interferometry of Abelian anyons include a more detailed modeling of the usual Fabry-Pérot setups, which accounts for competing effects [21] and the proposition of Hanbury Brown–Twiss interferometry to probe anyon correlations [22]. Building on earlier proposals [23], experiments pointing at non-Abelian properties were also performed [24]. Interferometric schemes for detecting the statistical phase were also developed for ultracold atomic [14] and photonic [17] systems. Recently, as a slightly different approach, proposals for detecting Haldane's fractional exclusion statistics [25], which is intimately connected to the braiding statistics, have appeared in the solid state [26], ultracold atomic [27], and photonic contexts [28].

In this Letter, we propose a much simpler time-of-flight (TOF) measurement [12] as a way to observe the statistical phase of an FQH liquid of ultracold atoms initially prepared in a quasihole state with Abelian braiding statistics. The suggested experimental procedure involves creating and pinning the quasiholes with localized potentials and suddenly releasing the atomic cloud to measure the density distribution after time of flight for one- and two-quasihole states. As the average total angular momentum of the initial state can be mathematically related both to the TOF mean square radius [29] and to the Berry phase [8,30] associated with quasihole braiding, a measurement of the former provides information on the latter quantity. As a key advantage over previous interferometric proposals [14,17], ours does not require physically moving quasiholes and is based on a standard TOF measurement on a static system.

Different, yet related aspects of the anyonic character of quasiholes have been addressed in recent works: the fractionalization of angular momentum has been discussed in [31] for test particles immersed in an ultracold atomic FQH system and, very recently, in [32] for impurities interacting with a bosonic bath. Signatures of anyonic statistics in the correlation functions of an expanding gas of anyons have been suggested in [33].

Model System.—We consider a generic FQH system with interacting neutral particles in a synthetic magnetic field B, which is uniform and perpendicular to the 2D plane of motion. Such a system, with N particles of mass M, can be described by the Hamiltonian

$$H_{\mathrm{FQH}} = \sum_{i=1}^{N} \frac{(-i\hbar\nabla_i - \mathbf{A})^2}{2M} + g_{\mathrm{int}} \sum_{i<j} \delta^{(2)}(\mathbf{r}_i - \mathbf{r}_j), \quad (1)$$

where $\mathbf{A}(\mathbf{r}) = B\hat{\mathbf{z}} \times \mathbf{r}/2$ is the synthetically created symmetric gauge vector potential. The strength of repulsive contact interactions is given by $g_{\mathrm{int}} > 0$.

The eigenstates of the noninteracting Hamiltonian are the Landau levels separated by the cyclotron energy $\Delta E = \hbar B/M$. When the typical interaction energy g_{int}/l_B^2, with $l_B = \sqrt{\hbar/B}$ the magnetic length, is sufficiently smaller than ΔE, it is reasonable to make the approximation that only the lowest Landau level (LLL) is occupied. The wave function of a single-particle eigenstate in the LLL with angular momentum $n\hbar$ is $\psi_n(\zeta) = \zeta^n e^{-|\zeta|^2/4}/(\sqrt{2\pi 2^n n!}\, l_B)$, where $\zeta = (x + iy)/l_B$ is the complex-valued coordinate of the particle.

For the many-particle system, one can define the filling fraction $\nu = N/N_\Phi$ as the ratio between the number of particles N and the number of magnetic flux quanta N_Φ, which corresponds to the filling of the Landau levels in the noninteracting case. For a fractional filling $\nu = 1/m$, the exact nondegenerate ground state of the interacting Hamiltonian H_{FQH} at a total angular momentum $\mathcal{L}_z = mN(N-1)\hbar/2$ is described by the Laughlin wave function [6,14,34]

$$\Psi_{\mathrm{FQH}}(\zeta_1, \ldots, \zeta_N) \propto \prod_{j<k} (\zeta_j - \zeta_k)^m e^{-\sum_{i=1}^{N} |\zeta_i|^2/4}, \quad (2)$$

where ζ_i is the complex-valued coordinate of the ith particle. For bosons (fermions) m must be even (odd) for the symmetry of the wave function to be correct. In what follows, we will focus on the two exemplary cases with $m = 2$ and 3. The $m = 3$ wave function is the ansatz proposed by Laughlin to describe the FQH effect for electrons at filling $\nu = 1/3$ [6]. The $m = 2$ bosonic wave function appeared, instead, in the context of rotating ultracold atoms [14,34,35] and was theoretically found to be the absolute ground state in the presence of a uniform synthetic magnetic field and a weak trapping potential [28,36]. In a similar setup with fermionic atoms, the ground state will be the $m = 3$ Laughlin state.

The Laughlin wave function (2) has zero-energy excitations known as quasiholes which obey anyonic exchange statistics in the thermodynamic limit [7,8]. When two quasiholes are exchanged, the many-body wave function acquires the phase $\phi_{\mathrm{st}} = \nu\pi$. Numerical studies show that quasiholes (qh) can be pinned by repulsive piercing potentials created with lasers in ultracold atomic systems [14,15]. Such a potential term can be represented by a sum of delta potentials as $V_{\mathrm{qh}} = V_0 \sum_{i=1}^{N_{\mathrm{qh}}} \sum_{j=1}^{N} \delta^{(2)}(\mathbf{r}_j - \mathbf{R}_i)$, where N_{qh} is the total number of repulsive potentials and $\mathbf{R}_i$ is the position of the ith localized potential with strength V_0.

According to exact diagonalization of small systems [37], the ground state of the total Hamiltonian $H_{\mathrm{qh}} = H_{\mathrm{FQH}} + V_{\mathrm{qh}} + V_{\mathrm{trap}}$ including suitable pinning and trapping [28,36] potentials is not affected by the details of the potentials and is well represented by the following one- and two-quasihole wave functions for $N_{\mathrm{qh}} = 1$ and 2, respectively,

$$\Psi_{1\mathrm{qh}}(\{\zeta_i\}, \mathcal{R}_1) \propto \prod_{i=1}^{N} (\zeta_i - \mathcal{R}_1) \Psi_{\mathrm{FQH}}(\zeta_1, \ldots, \zeta_N), \quad (3)$$

$$\Psi_{2\mathrm{qh}}(\{\zeta_i\}, \{\mathcal{R}_j\}) \propto \prod_{i=1}^{N} \prod_{j=1}^{2} (\zeta_i - \mathcal{R}_j) \Psi_{\mathrm{FQH}}(\zeta_1, \ldots, \zeta_N), \quad (4)$$

where $\mathcal{R}_{1,2}$ are the complex positions of the quasiholes determined by the positions $\mathbf{R}_{1,2}$ of the localized potentials. From the experimental perspective, once the ultracold atomic cloud is prepared in the Laughlin ground state, which is assumed to be sufficiently separated from both the gapped bulk excitations and low-lying edge excitations so that thermal fluctuations do not spoil it, one can adiabatically prepare the quasihole states by slowly increasing the strength V_0 of the repulsive potentials and then slowly moving them to the desired position in space [14]. Alternatively, one may also consider directly cooling down the gas in the presence of the potentials.

Braiding phase and total angular momentum.—In our system with quasiholes, the braiding phase corresponds to the difference between the Berry phases the many-body wave function acquires after a quasihole is moved along a closed path with or without another quasihole enclosed by the path [7,8]. Provided the quasiholes remain sufficiently far apart from each other, the braiding phase does not depend on the details of the path; therefore, we can consider a circular path of radius R, cyclically parametrized by the angular coordinate θ. We further assume that the second quasihole (if present) is pinned at the origin. The Berry phase [30], in this case, becomes

$$\varphi_B(R) = i \oint_R \langle \Psi(\theta) | \partial_\theta | \Psi(\theta) \rangle d\theta, \quad (5)$$

where $|\Psi(\theta)\rangle$ refers to the one- or two-quasihole states (3)–(4).

We now relate the Berry phase (5) to the expected value of total angular momentum $\langle L_z \rangle$, by first writing the action of the partial derivative ∂_θ on the state $|\Psi(\theta)\rangle$ as

$\partial_\theta|\Psi(\theta)\rangle = \lim_{\delta\theta\to 0}\{[|\Psi(\theta+\delta\theta)\rangle - |\Psi(\theta)\rangle]/\delta\theta\}$. Since rotating the quasihole by $\delta\theta$ is equivalent to rotating the whole many-body system by the same angle (modulo a 2π-periodic phase factor, linearly dependent on $\delta\theta$), the state $|\Psi(\theta+\delta\theta)\rangle$ can be represented using the rotation generator L_z as $|\Psi(\theta+\delta\theta)\rangle = \exp(-iL_z\delta\theta/\hbar)|\Psi(\theta)\rangle$. Expanding the rotation operator for small $\delta\theta$ as $\exp(-iL_z\delta\theta/\hbar) \simeq 1 - iL_z\delta\theta/\hbar$, we see that $\partial_\theta|\Psi(\theta)\rangle = -(iL_z/\hbar)|\Psi(\theta)\rangle$, which implies

$$\varphi_B(R) = \frac{1}{\hbar}\oint_R \langle\Psi(\theta)|L_z|\Psi(\theta)\rangle d\theta = \frac{2\pi}{\hbar}\langle L_z\rangle, \qquad (6)$$

where the expectation value of $\langle L_z\rangle$ is taken with respect to a wave function having a quasihole with fixed radial coordinate R but an arbitrary angular coordinate. This remarkable expression relates a quantity resulting from an adiabatic motion, that is, braiding, to a stationary property of a quantum mechanical state, that is, the average total angular momentum [40].

Equation (6) also provides an experimental route for measuring the braiding (br) phase given by the Berry phase differences $\phi_{\rm br}(R) = \varphi_B^{\rm 2qh}(R) - \varphi_B^{\rm 1qh}(R)$ yielding

$$\phi_{\rm br}(R) = \frac{2\pi}{\hbar}\left(\langle L_z\rangle^{\rm 2qh} - \langle L_z\rangle^{\rm 1qh}\right), \qquad (7)$$

where the superscripts 1qh and 2qh refer to one- and two-quasihole states, respectively. Equation (7) shows that the braiding phase can simply be determined by measuring the average total angular momentum for two quantum states and taking the difference, without any need to actually braid quasiholes. The fact that the braiding phase is defined in Eq. (7) only up to an integral multiple of 2π does not preclude highlighting the fractional statistics.

As an alternative to the braiding phase, one may choose to directly measure the statistical (st) phase $\phi_{\rm st}(R) = \phi_{\rm br}(R)/2$ involving the adiabatic exchange of two quasiholes [15,17]. In our proposal, this would correspond to measuring the angular momentum in the two cases of (a) two quasiholes pinned at diametrically opposite positions each at a distance $R/2$ from the origin and (b) a single quasihole pinned at a radius $R/2$. In particular, one can write

$$\phi_{\rm st}(R) = \frac{\pi}{\hbar}\left(\langle L_z\rangle^{\rm 2qh}_{\rm op} - 2\langle L_z\rangle^{\rm 1qh}\right) + \pi m\frac{N(N-1)}{2}, \qquad (8)$$

where $\langle L_z\rangle^{\rm 2qh}_{\rm op}$ is the average total angular momentum of the two-quasihole state with diametrically opposite (op) quasiholes and the last term compensates the phase factor picked up by the quasihole wave functions after a π rotation [41]. Although we will evaluate the statistical phase only for the case of oppositely located quasiholes, Eq. (8) can be generalized to configurations in which quasiholes are pinned at generic positions. However, such a generalization requires three different measurements of $\langle L_z\rangle$, instead of two [41].

Time-of-flight measurement.—The average total angular momentum of a cloud of cold atoms occupying the LLL can be determined by just measuring the mean square radius $\langle r^2\rangle$ of the density distribution of atoms in the trap or, even easier, after a time-of-flight expansion for a duration t once the pinning and trapping potentials and synthetic fields are suddenly turned off [29,42]

$$\langle r^2\rangle_{\rm TOF} = \frac{1}{N}\left(\frac{\hbar t}{\sqrt{2}Ml_B}\right)^2\left(\frac{\langle L_z\rangle}{\hbar} + N\right) = \left(\frac{\hbar t}{2Ml_B^2}\right)^2\langle r^2\rangle. \qquad (9)$$

Note that for this self-similar TOF expansion to be valid, the interactions between particles should be negligible during the expansion, but the initial state can well be a highly correlated one. This omission of interaction effects can be justified, for instance, whenever the system can be described within the LLL approximation [46].

Combining Eq. (7) with the relation displayed in Eq. (9) between the in-trap average total angular momentum $\langle L_z\rangle$ and $\langle r^2\rangle_{\rm TOF}$, we obtain the fundamental experimental observable yielding the braiding phase

$$\phi_{\rm br}(R) \simeq 2\pi N\left(\frac{\sqrt{2}Ml_B}{\hbar t}\right)^2\left(\langle r^2\rangle^{\rm 2qh}_{\rm TOF} - \langle r^2\rangle^{\rm 1qh}_{\rm TOF}\right), \qquad (10)$$

which is, again, defined up to an integral multiple of 2π. Similarly, the corresponding observable for $\phi_{\rm st}(R)$ can be found by using Eqs. (8) and (9).

Numerical Results.—In this section, we substantiate our conclusions by presenting estimates for $\phi_{\rm br}(R)$ calculating the in-trap mean square radius $\langle r^2\rangle$, related to $\langle r^2\rangle_{\rm TOF}$ through Eq. (9). Our numerical calculations are based on the analytical wave functions (3)–(4) and we use a Monte Carlo (MC) technique [47] to compute $\langle r^2\rangle$ and the density profile [48]. As a further check, we performed exact diagonalization calculations for smaller N so as to benchmark the MC results and verify that the ground state wave functions for suitable pinning and trapping potentials match the analytical wave functions [37].

We consider two configurations of two-quasihole states, where the distance between two quasiholes is denoted by $R = |\mathbf{R}_1 - \mathbf{R}_2|$ in each case. In Fig. 1, one of the quasiholes is located at the center, so we calculate $\phi_{\rm br}(R) = 2\pi N(\langle r^2\rangle^{\rm 2qh} - \langle r^2\rangle^{\rm 1qh})/(\sqrt{2}l_B)^2$ determined by Eqs. (7) and (9). In Fig. 2, two quasiholes are located at diametrically opposite positions, so the relevant quantity is $\phi_{\rm st}(R) = \pi N(\langle r^2\rangle^{\rm 2qh}_{\rm op} - 2\langle r^2\rangle^{\rm 1qh})/(\sqrt{2}l_B)^2 + \pi N + \pi mN(N-1)/2$ from Eqs. (8) and (9).

In the calculations for $N = 20$-particle systems shown in Fig. 1(a), a clear plateau is seen for $\nu = 1/2$ at the expected

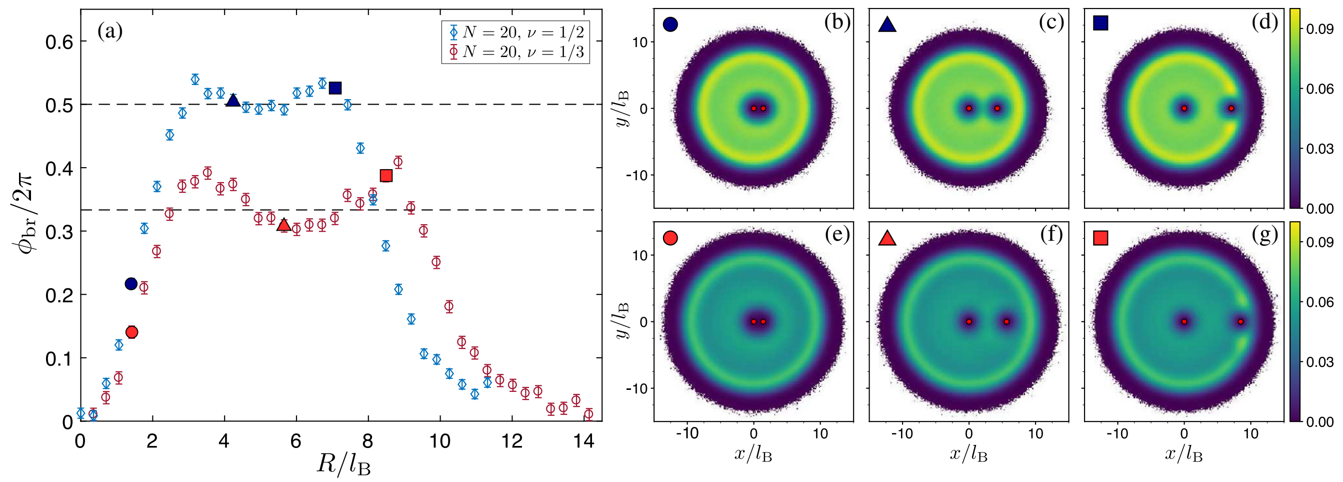

FIG. 1. (a) Quasihole braiding phase ϕ_{br} as a function of the distance $R = |\mathbf{R}_1 - \mathbf{R}_2|$ between two quasiholes for systems of $N = 20$ particles at filling $\nu = 1/2$ (blue diamonds) and $\nu = 1/3$ (red circles), where one of the quasiholes is fixed in the origin ($|\mathbf{R}_2| = 0$). Error bars represent statistical uncertainties on the data. Density profiles characterizing some two-quasihole states are given for $\nu = 1/2$ in (b)–(d) and for $\nu = 1/3$ in (e)–(g). The position of the outer quasihole is fixed along the x axis at $x_1/\sqrt{2}l_B = 1,\ 3,\ 5$ in (b)–(d) and at $x_1/\sqrt{2}l_B = 1,\ 4,\ 6$ in (e)–(g).

fractional value $\phi_{\mathrm{br}}/2\pi = 1/2$, accompanied by small bumps at its ends. These bumps are more pronounced in the $\nu = 1/3$ case, where the plateau is not fully visible, and can be related to perturbations in the FQH cloud density.

On one hand, at small R [filled circles in Fig. 1(a)], the phase behavior reflects the density deformation induced by the quasihole in the origin shown in Figs. 1(b) and 1(e). Such a deformation is not sensitive to the cloud size that increases with N and directly reflects the size of the quasihole. Especially for $\nu = 1/3$ the bump in $\phi_{\mathrm{br}}(R)$ precisely matches the position of the peak in the density profile [52–54]. On the other hand, the bump visible at large R [filled squares in Fig. 1(a)] is related to the density increase in the vicinity of the cloud edge [Figs. 1(d) and 1(g)]. The scaling of the bump position with N and that of the bump visibility with ν confirm the behavior of the density maximum: the former scales as $\sqrt{N}$, while the latter increases with decreasing ν.

While smaller clouds give qualitatively similar results albeit with quantitatively more pronounced deviations, these calculations prove that, for $\nu = 1/2$, an $N = 20$-particle system is already big enough to properly measure the anyonic statistics of quasiholes. On the other hand, for $\nu = 1/3$, the bigger effective size of quasiholes requires larger systems to clearly observe the plateau in the braiding phase. Since larger particle numbers typically require a higher relative precision in measuring the angular momentum, a useful alternative option is to consider the second configuration with quasiholes at diametrically opposite positions [15,17]: such a configuration allows us to maximize the quasihole distance by exploiting the full extension of the bulk region. In this way, it is possible to obtain a clear plateau in the statistical phase also for $\nu = 1/3$ and $N = 20$ particles, as displayed in Fig. 2(a).

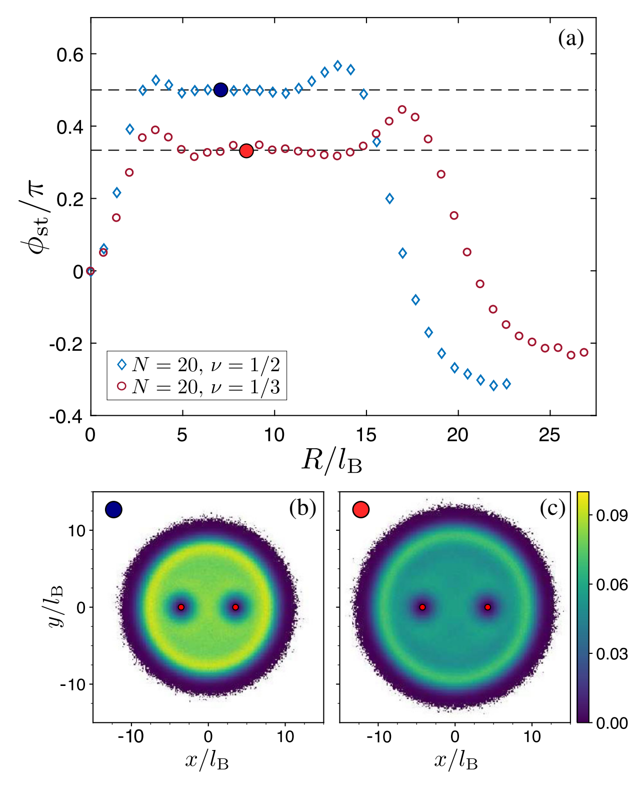

FIG. 2. (a) Statistical phase ϕ_{st} as a function of the distance $R = |\mathbf{R}_1 - \mathbf{R}_2|$ between two quasiholes for systems of $N = 20$ particles at filling $\nu = 1/2$ (blue diamonds) and $\nu = 1/3$ (red circles), where the quasiholes are located at diametrically opposite positions ($x_1 = -x_2 = R/2$). Error bars are smaller than the symbol size. (b) Density profile for $\nu = 1/2$ with quasiholes located along the x axis at $x_1 = -x_2 = 2.5\sqrt{2}l_B$. (c) Density profile for $\nu = 1/3$ with quasiholes located along the x axis at $x_1 = -x_2 = 3\sqrt{2}l_B$.

Conclusion.—In this Letter, we argued that a standard measurement of the static density profile in the trap or after time of flight is sufficient to observe the anyonic statistics of quasiholes in a gas of ultracold atoms in the FQH regime. We showed that the mean square radius of the cloud in the presence of one or two quasiholes is directly related to the braiding and statistical phases. Numerical calculations of the braiding phase $\phi_{\rm br}$ as a function of the distance between quasiholes for a reasonable number of particles ($N = 20$) clearly display a plateau region, for which the quasiholes are sufficiently far away from each other and from the edge of the cloud. Except for small finite-size deviations, the value of the plateau is very close to the expected one $\phi_{\rm st} = \phi_{\rm br}/2 = \nu\pi$, giving a clear signature of the quasihole anyonic statistics.

A possible extension of our protocol to the case of non-Abelian anyons is also the subject of ongoing studies. The key difference is that the Berry phase is replaced by its Wilczek-Zee generalization [5], which depends on a matrix of inner products of the form $\langle\Psi_\alpha(\theta)|\partial_\theta|\Psi_\beta(\theta)\rangle$. Indices α and β label the degenerate quasihole ground states peculiar to non-Abelian phases. In order to generalize our scheme, we will first need to verify the identification of $\partial_\theta|\Psi_\alpha(\theta)\rangle$ with $L_z|\Psi_\alpha(\theta)\rangle$ and then to connect the angular momentum matrix elements $\langle\Psi_\alpha(\theta)|L_z|\Psi_\beta(\theta)\rangle$ with certain real-space observables like $\langle r^2\rangle$ considered in the current Letter. Such a real-space approach might be appealing, particularly in view of the possibility of using a generalized plasma analogy [55]. From the perspective of reproducing our proposal in the non-Abelian context, it looks promising to consider the $p_x + ip_y$ model of topological superconductors [5], as the Moore-Read state [56], representing the simplest FQH state with non-Abelian statistics, can be described through the p-wave pairing of composite fermions [57].

Further work will extend these results to FQH liquids of photons in cylindrical set-ups such as the twisted resonators of [58], for which the far-field intensity profile of the light emission provides the optical analog of time-of-flight imaging of ultracold atomic clouds. A first task will be to identify suitable schemes to generate stable quasiholes states, e.g., by generalizing the frequency-dependent incoherent pumping scheme of [28] in the presence of pinning potentials piercing the cavity. We then expect that the braiding phase of quasiholes can again be extracted from the expectation value of the angular momentum.

This work was supported by the EU-FET Proactive Grant No. AQuS, Project No. 640800, and by the Autonomous Province of Trento, partially through the project "On silicon chip quantum optics for quantum computing and secure communications." Discussions with N. Cooper, L. Mazza, T. Ozawa, H. M. Price, and R. Santachiara are warmly acknowledged.

[1] J. M. Leinaas and J. Myrheim, On the theory of identical particles, Nuovo Cimento B **37**, 1 (1977).
[2] Y.-S. Wu, General Theory for Quantum Statistics in Two Dimensions, Phys. Rev. Lett. **52**, 2103 (1984).
[3] A. Stern, Anyons and the quantum Hall effect—A pedagogical review, Ann. Phys. (Amsterdam) **323**, 204 (2008).
[4] F. Wilczek, Quantum Mechanics of Fractional-Spin Particles, Phys. Rev. Lett. **49**, 957 (1982).
[5] C. Nayak, S. H. Simon, A. Stern, M. Freedman, and S. Das Sarma, Non-Abelian anyons and topological quantum computation, Rev. Mod. Phys. **80**, 1083 (2008).
[6] R. B. Laughlin, Anomalous Quantum Hall Effect: An Incompressible Quantum Fluid with Fractionally Charged Excitations, Phys. Rev. Lett. **50**, 1395 (1983).
[7] D. Yoshioka, *The Quantum Hall Effect* (Springer-Verlag, Berlin, 2002).
[8] D. Arovas, J. R. Schrieffer, and F. Wilczek, Fractional Statistics and the Quantum Hall Effect, Phys. Rev. Lett. **53**, 722 (1984).
[9] D. C. Tsui, H. L. Stormer, and A. C. Gossard, Two-Dimensional Magnetotransport in the Extreme Quantum Limit, Phys. Rev. Lett. **48**, 1559 (1982).
[10] N. Goldman, G. Juzeliūnas, P. Öhberg, and I. B. Spielman, Light-induced gauge fields for ultracold atoms, Rep. Prog. Phys. **77**, 126401 (2014); J. Dalibard, F. Gerbier, G. Juzeliūnas, and P. Öhberg, Colloquium: Artificial gauge potentials for neutral atoms, Rev. Mod. Phys. **83**, 1523 (2011).
[11] A. B. Khanikaev and G. Shvets, Two-dimensional topological photonics, Nat. Photonics **11**, 763 (2017); L. Lu, J. D. Joannopoulos, and M. Soljačić, Topological photonics, Nat. Photonics **8**, 821 (2014).
[12] I. Bloch, J. Dalibard, and W. Zwerger, Many-body physics with ultracold gases, Rev. Mod. Phys. **80**, 885 (2008).
[13] I. Carusotto and C. Ciuti, Quantum fluids of light, Rev. Mod. Phys. **85**, 299 (2013).
[14] B. Paredes, P. Fedichev, J. I. Cirac, and P. Zoller, 1/2-Anyons in Small Atomic Bose-Einstein Condensates, Phys. Rev. Lett. **87**, 010402 (2001).
[15] T. Graß, B. Juliá-Díaz, and M. Lewenstein, Topological phases in small quantum Hall samples, Phys. Rev. A **89**, 013623 (2014); B. Juliá-Díaz, T. Graß, N. Barberán, and M. Lewenstein, Fractional quantum Hall states of a few bosonic atoms in geometric gauge fields, New J. Phys. **14**, 055003 (2012).
[16] R. O. Umucalılar and I. Carusotto, Many-body braiding phases in a rotating strongly correlated photon gas, Phys. Lett. A **377**, 2074 (2013).
[17] S. Dutta and E. J. Mueller, Coherent generation of photonic fractional quantum Hall states in a cavity and the search for anyonic quasiparticles, Phys. Rev. A **97**, 033825 (2018).
[18] J. Martin, S. Ilani, B. Verdene, J. Smet, V. Umansky, D. Mahalu, D. Schuh, G. Abstreiter, and A. Yacoby, Localization of fractionally charged quasi-particles, Science **305**, 980 (2004); R. de-Picciotto, M. Reznikov, M. Heiblum, V. Umansky, G. Bunin, and D. Mahalu, Direct observation of a fractional charge, Nature (London) **389**, 162 (1997); L. Saminadayar, D. C. Glattli, Y. Jin, and B. Etienne, Observation of the $e/3$ Fractionally Charged Laughlin Quasiparticle, Phys. Rev. Lett. **79**, 2526 (1997); V. J. Goldman and B. Su, Resonant tunneling in the quantum Hall regime:

Measurement of fractional charge, Science **267**, 1010 (1995).

[19] F. E. Camino, W. Zhou, and V. J. Goldman, Realization of a Laughlin quasiparticle interferometer: Observation of fractional statistics, Phys. Rev. B **72**, 075342 (2005); F. E. Camino, W. Zhou, and V. J. Goldman, Aharonov-Bohm Superperiod in a Laughlin Quasiparticle Interferometer, Phys. Rev. Lett. **95**, 246802 (2005).

[20] B. Rosenow and B. I. Halperin, Influence of Interactions on Flux and Back-Gate Period of Quantum Hall Interferometers, Phys. Rev. Lett. **98**, 106801 (2007); V. J. Goldman, Superperiods and quantum statistics of Laughlin quasiparticles, Phys. Rev. B **75**, 045334 (2007); E.-A. Kim, Aharanov-Bohm Interference and Fractional Statistics in a Quantum Hall Interferometer, Phys. Rev. Lett. **97**, 216404 (2006); J. K. Jain and C. Shi, Resonant Tunneling in the Fractional Quantum Hall Effect: Superperiods and Braiding Statistics, Phys. Rev. Lett. **96**, 136802 (2006).

[21] B. I. Halperin, A. Stern, I. Neder, and B. Rosenow, Theory of the Fabry-Pérot quantum Hall interferometer, Phys. Rev. B **83**, 155440 (2011).

[22] G. Campagnano, O. Zilberberg, I. V. Gornyi, D. E. Feldman, A. C. Potter, and Y. Gefen, Hanbury Brown–Twiss Interference of Anyons, Phys. Rev. Lett. **109**, 106802 (2012).

[23] A. Stern and B. I. Halperin, Proposed Experiments to Probe the Non-Abelian $\nu = 5/2$ Quantum Hall State, Phys. Rev. Lett. **96**, 016802 (2006); P. Bonderson, A. Kitaev, and K. Shtengel, Detecting Non-Abelian Statistics in the $\nu = 5/2$ Fractional Quantum Hall State, Phys. Rev. Lett. **96**, 016803 (2006).

[24] R. L. Willett, L. N. Pfeiffer, and K. W. West, Alternation and interchange of $e/4$ and $e/2$ period interference oscillations consistent with filling factor 5/2 non-Abelian quasiparticles, Phys. Rev. B **82**, 205301 (2010).

[25] F. D. M. Haldane, "Fractional Statistics" in Arbitrary Dimensions: A Generalization of the Pauli Principle, Phys. Rev. Lett. **67**, 937 (1991).

[26] Z. Papić, R. S. K. Mong, A. Yazdani, and M. P. Zaletel, Imaging Anyons with Scanning Tunneling Microscopy, Phys. Rev. X **8**, 011037 (2018).

[27] N. R. Cooper and S. H. Simon, Signatures of Fractional Exclusion Statistics in the Spectroscopy of Quantum Hall Droplets, Phys. Rev. Lett. **114**, 106802 (2015).

[28] R. O. Umucalılar and I. Carusotto, Generation and spectroscopic signatures of a fractional quantum Hall liquid of photons in an incoherently pumped optical cavity, Phys. Rev. A **96**, 053808 (2017).

[29] T.-L. Ho and E. J. Mueller, Rotating Spin-1 Bose Clusters, Phys. Rev. Lett. **89**, 050401 (2002).

[30] M. V. Berry, Quantal phase factors accompanying adiabatic changes, Proc. R. Soc. A **392**, 45 (1984).

[31] Y. Zhang, G. J. Sreejith, and J. K. Jain, Creating and manipulating non-Abelian anyons in cold atom systems using auxiliary bosons, Phys. Rev. B **92**, 075116 (2015); Y. Zhang, G. J. Sreejith, N. D. Gemelke, and J. K. Jain, Fractional Angular Momentum in Cold-Atom Systems, Phys. Rev. Lett. **113**, 160404 (2014).

[32] E. Yakaboylu and M. Lemeshko, Anyonic statistics of quantum impurities in two dimensions, arXiv:1712.00308.

[33] T. Dubček, B. Klajn, R. Pezer, H. Buljan, and D. Jukić, Quasimomentum distribution and expansion of an anyonic gas, Phys. Rev. A **97**, 011601(R) (2018).

[34] N. R. Cooper, N. K. Wilkin, and J. M. F. Gunn, Quantum Phases of Vortices in Rotating Bose-Einstein Condensates, Phys. Rev. Lett. **87**, 120405 (2001); N. K. Wilkin and J. M. F. Gunn, Condensation of "Composite Bosons" in a Rotating BEC, Phys. Rev. Lett. **84**, 6 (2000); N. R. Cooper and N. K. Wilkin, Composite fermion description of rotating Bose-Einstein condensates, Phys. Rev. B **60**, R16279(R) (1999).

[35] N. R. Cooper, Rapidly rotating atomic gases, Adv. Phys. **57**, 539 (2008).

[36] R. Fern and S. H. Simon, Quantum Hall edges with hard confinement: Exact solution beyond Luttinger liquid, Phys. Rev. B **95**, 201108(R) (2017); E. Macaluso and I. Carusotto, Hard-wall confinement of a fractional quantum Hall liquid, Phys. Rev. A **96**, 043607 (2017).

[37] See Supplemental Material at http://link.aps.org/supplemental/10.1103/PhysRevLett.120.230403, which includes Refs. [38,39], for the details of the exact diagonalization results.

[38] B. A. Bernevig and F. D. M. Haldane, Model Fractional Quantum Hall States and Jack Polynomials, Phys. Rev. Lett. **100**, 246802 (2008).

[39] E. Macaluso and I. Carusotto, Ring-shaped fractional quantum Hall liquids with hard-wall potentials, arXiv:1804.07563.

[40] This result was obtained in [16] for the special case when the many-body wave function can be written in the LLL. The same relation has appeared in a different system investigated in [32].

[41] See Supplemental Material at http://link.aps.org/supplemental/10.1103/PhysRevLett.120.230403 for a discussion of the additional term in the statistical phase and for results involving generic quasihole positions.

[42] See Supplemental Material at http://link.aps.org/supplemental/10.1103/PhysRevLett.120.230403, which includes Refs. [12,29,43–46], for the relation between time-of-flight and in-trap averages.

[43] I. S. Gradshteyn and I. M. Ryzhik, *Tables of Integrals, Series, and Products*, 4th ed. (Academic Press, New York, 1980).

[44] C. Cohen-Tannoudji, B. Diu, and F. Laloë, *Quantum Mechanics* (Wiley, New York, 1977).

[45] M. Andrews, The evolution of oscillator wave functions, Am. J. Phys. **84**, 270 (2016).

[46] N. Read and N. R. Cooper, Free expansion of lowest-Landau-level states of trapped atoms: A wave-function microscope, Phys. Rev. A **68**, 035601 (2003).

[47] T. Comparin and E. Macaluso, TCOMPA/LAUGHLIN-METROPOLIS, https://doi.org/10.5281/zenodo.1161969.

[48] See Supplemental Material at http://link.aps.org/supplemental/10.1103/PhysRevLett.120.230403, which includes Refs. [49–52], for the details of the Monte Carlo calculation.

[49] N. Metropolis, A. W. Rosenbluth, M. N. Rosenbluth, A. H. Teller, and E. Teller, Equation of state calculations by fast computing machines, J. Chem. Phys. **21**, 1087 (1953).

[50] W. Krauth, *Statistical Mechanics: Algorithms and Computations* (Oxford University Press, Oxford, 2006).

[51] H. Kjønsberg and J. Myrheim, Numerical study of charge and statistics of Laughlin quasiparticles, Int. J. Mod. Phys. A **14**, 537 (1999).

[52] R. Morf and B. I. Halperin, Monte Carlo evaluation of trial wave functions for the fractional quantized Hall effect: Disk geometry, Phys. Rev. B **33**, 2221 (1986).

[53] A. C. Balram, Y.-H. Wu, G. J. Sreejith, A. Wójs, and J. K. Jain, Role of Exciton Screening in the 7/3 Fractional Quantum Hall Effect, Phys. Rev. Lett. **110**, 186801 (2013).

[54] S. Johri, Z. Papić, R. N. Bhatt, and P. Schmitteckert, Quasiholes of $\frac{1}{3}$ and $\frac{7}{3}$ quantum Hall states: Size estimates via exact diagonalization and density-matrix renormalization group, Phys. Rev. B **89**, 115124 (2014).

[55] V. Gurarie and C. Nayak, A plasma analogy and Berry matrices for non-Abelian quantum Hall states, Nucl. Phys. **B506**, 685 (1997); P. Bonderson, V. Gurarie, and C. Nayak, Plasma analogy and non-Abelian statistics for Ising-type quantum Hall states, Phys. Rev. B **83**, 075303 (2011).

[56] G. Moore and N. Read, Non-Abelions in the fractional quantum hall effect, Nucl. Phys. **B360**, 362 (1991).

[57] G. Möller and S. H. Simon, Paired composite-fermion wave functions, Phys. Rev. B **77**, 075319 (2008).

[58] N. Schine, A. Ryou, A. Gromov, A. Sommer, and J. Simon, Synthetic Landau levels for photons, Nature (London) **534**, 671 (2016).